Results in Physics 9 (2018) 625–627

Contents lists available at ScienceDirect

Results in Physics

journal homepage: www.journals.elsevier.com/results-in-physics

Brillouin lasing in single-mode tapered optical fiber with inscribed fiber Bragg grating array

S.M. Popov [a,*], O.V. Butov [a], Y.K. Chamorovskiy [a,b], V.A. Isaev [a], A.O. Kolosovskiy [a], V.V. Voloshin [a], I.L. Vorob'ev [a], M.Yu. Vyatkin [a], P. Mégret [c], M. Odnoblyudov [b], D.A. Korobko [d], I.O. Zolotovskii [d], A.A. Fotiadi [c,d,e]

[a] Institute of Radio Engineering and Electronics (Fryazino Branch), Russian Academy of Science, Vvedenskogo Sq. 1, 141190 Fryazino, Moscow Region, Russian Federation
[b] Peter the Great St. Petersburg Polytechnic University, Politekhnicheskaya 29, 195251 St. Petersburg, Russian Federation
[c] Electromagnetism and Telecommunication Department, University of Mons, 31 Boulvard Dolez, Mons 7000, Belgium
[d] Ulyanovsk State University, 42 Leo Tolstoy Street, Ulyanovsk 432970, Russian Federation
[e] Ioffe Physico-Technical Institute of the Russian Academy of Sciences, 26 Polytekhnicheskaya Street, St. Petersburg 194021, Russian Federation

ARTICLE INFO

Article history:
Received 24 December 2017
Received in revised form 12 March 2018
Accepted 12 March 2018
Available online 16 March 2018

Keywords:
Tapered optical fibers
Fiber Bragg gratings
Random lasers

ABSTRACT

A tapered optical fiber has been manufactured with an array of fiber Bragg gratings (FBG) inscribed during the drawing process. The total fiber peak reflectivity is 5% and the reflection bandwidth is ~3.5 nm. A coherent frequency domain reflectometry has been applied for precise profiling of the fiber core diameter and grating reflectivity both distributed along the whole fiber length. These measurements are in a good agreement with the specific features of Brillouin lasing achieved in the semi-open fiber cavity configuration.

Fiber Bragg Gratings (FBGs) are commonly used as sensors of physical quantities (temperature, mechanical tension, light polarization state, etc.) [1,2]. Another promising FBG application is spectral filtering employed in complex optical processing systems [3]. In the latter case the use of FBG arrays inscribed in a single fiber is of particular interest for processing of broadband signals. The problem of technical realization of such FBGs array fibers is on the agenda. One of the ways to produce an FBGs array with a broadband reflectivity is smart modification of the fiber diameter along the fiber length before or after FBG inscription. Such variation causes a change of the mode effective refractive index n_{eff} that directly sets the distribution of the FBG peak reflectivity wavelength $\lambda = n_{\text{eff}}\Lambda/2$ along the fiber length, where Λ is the period of the phase mask. For an example, in Ref. [4] an uniform FBG inscribed in an optical fiber with the diameter of 125 μm has been modified by smooth tapering of the fiber diameter down to 10 μm leading to 10 fold broadening of the FBG reflectivity spectrum. In that experiment a thermal heating up to the glass melting temperature with simultaneous stretching of the fiber have been applied for fiber tapering. A similar effect has been reported as well for etching optical fiber with an pre-inscribed uniform FBG [5]. The main limitations of the mentioned techniques are a small number of FBGs inscribed in a single fiber, degradation of FBG quality during heating, a short physical length of the FBG array fiber, significant linear losses. Recently, we have demonstrated an uniform FBG arrays [6,7] recorded in an optical fiber by an excimer laser operating at 248 nm immediately during the drawing process. Such a fiber containing up to 10,000 FBGs has a typical lengths of hundreds of meters and exhibit the reflectivity spectrum width of ~0.2 nm. Our inscription technique in combination with the possibility to control the fiber diameter during the drawing process allows to produce FBGs arrays possessing the reflectivity distributed along hundreds of meters, i.e. over the whole optical fiber length. Such a new all fiber device is of great interest for many photonic applications, like optical signal processing, distributed fiber sensing, random fiber lasers.

In this paper, an optical fiber has been drawn with a speed of ~6 m/min from an isotropic optical fiber preform manufactured with a photosensitive $GeO_2 - B - SiO_2$ core. Multiple FBGs have been inscribed in the fiber one-by-one through a phase mask (the mask period is 1070 nm, the phase mask base is 10 mm) immediately during the drawing process and the outer diameter of the fiber has been precisely controlled by the preform feed

* Corresponding author.
E-mail address: sergei@popov.eu.org (S.M. Popov).

https://doi.org/10.1016/j.rinp.2018.03.023
2211-3797/

and is managed to change linearly with the fiber length. The resulting fiber parameters are the following: the core diameter is ~6 μm, the core/cladding refraction index difference is ~0.025, the cutoff wavelength is ~1350 nm (for outer diameter of 125 μm). The length of the experimental optical fiber sample is ~85 m. Along the fiber the outer diameter changes linearly with the fiber length from ~125 down to ~80 μm and then from ~80 down to ~125 μm. A total number of FBGs inscribed in the fiber sample is ~4250.

The fiber sample has been tested with an optical frequency domain reflectometry (OFDR) analyzer (OBR-4600, Luna) [8–12], and a spectral analyzer (AQ6370D, Yokogawa). The distributions of the fiber outer diameter and the local peak reflectivity wavelength along the fiber length are shown in Fig. 1 (a) by black and blue curves, respectively. One can see that a decrease of the fiber diameter from 125 μm down to 80 μm causes synchronous changes of the peak reflectivity wavelength from 1551.5 nm down to 1548 nm. Small difference between two profiles is explained by natural inhomogeneity of preform (refractive index fluctuations). The optical transmittance and reflectivity spectra are shown at Fig. 1 (b). One can see that the coefficients of reflection and transmission are not uniform over the spectrum. The reflection coefficient is lower at shorter peak reflectivity wavelengths corresponding to smaller optical fiber diameter. This feature could be explained by smaller fraction of the optical power propagating within the core of smaller size and so interacting with the inscribed FBG with lower efficiency.

To achieve Brillouin lasing in the tapered FBGs array fiber [13] a narrow-band laser source (~100 kHz, Agilent) coupled with an erbium doped amplifier (EDFA) and tunable between 1547 and 1553 nm has been used as a pump source. The FBGs array fiber sample is attached to the laser source through an optical circulator and is attached to a broadband mirror with the reflectivity of ~85% (Fig. 2(a)). The use of the broadband mirror makes possible two directional pumping of Brillouin cavity providing amplification not only for backward, but also for forward Brillouin Stokes waves. Such bidirectional pumping significantly decreases the lasing threshold. The output Brillouin laser radiation measured through the circulator output is up-shifted in respect to the pump wavelength by ~0.09 nm that corresponds to the SBS shift of 11 GHz (Fig. 1(b)) [14]. A narrow band FBG (~70 pm) attached to the circulator filters out the residual pump power.

In our experiment the lasing is achieved in semi-open fiber cavity configuration [15] due to backreflection from the mirror and backscattering from the FBG array fiber. The position inside the fiber, where an efficient backscattering occurs is determined by the position of FBG with the reflectivity spectral peak matching the peak of the Brillouin gain spectrum that in its turn is determined by the pumping wavelength. Therefore, the effective laser cavity is confined between the cavity mirror and this particular FBG. Tuning of the pumping wavelength in the range between 1548 and 1552 nm causes the corresponding shifts of Brillouin gain spectrum and the point inside the fiber, where the most efficient backscattering occurs thus leading to the corresponding change of the laser cavity length. The dependences of the output power on the pump power for different pump wavelengths are shown in Fig. 2(b). The minimum and maximal lasing threshold of ~75mW and ~320mW are achieved at 1551.31 nm and 1548.62 nm pumping wavelengths, respectively, that correspond to the longest and shortest laser cavity lengths as shown in Fig. 1(a). A typical self-heterodyne laser spectrum recorded for the pump wavelength of ~1551.31 nm is presented in Fig. 2(c). The spectrum is measured by RF analyzer (FSVR13, Rohde & Schwarz) employing an unbalanced Mach-Zehnder interferometer with the optical path difference of 25 km and comprising ~110 MHz electro-optic modulator. The recorded spectrum consists of the central peak with ~100 kHz width and multiple side-band peaks equally-spaced with the period of $\Delta f \sim 1.3$ MHz. One could check that this period is directly linked to the Brillouin cavity length as $L = c/2n\Delta f$ determined by a distance between the cavity mirror and the particular FBGs matching the peak of the Brillouin gain spectrum. Fig. 2(d) shows the dependence of the spacing period Δf on the pumping wavelength. The values of a Brillouin cavity length L calculated from the measured Δf for different lasing wavelengths are presented in Fig. 2(d) and marked in Fig. 1(a) by red lines. One can see that they are in a good agreement with the FBG peak wavelength distribution shown in Fig. 1(a).

The technology enabling manufacturing of the tapered FBG array fiber has been developed and applied for production of the 85 m-fiber sample. The fiber possesses properties attractive for photonic techniques (optical information processing, fiber temperature distributed sensors, random fiber lasers, distributed feedback lasers). Brillouin lasing demonstrated for a semi-open cavity

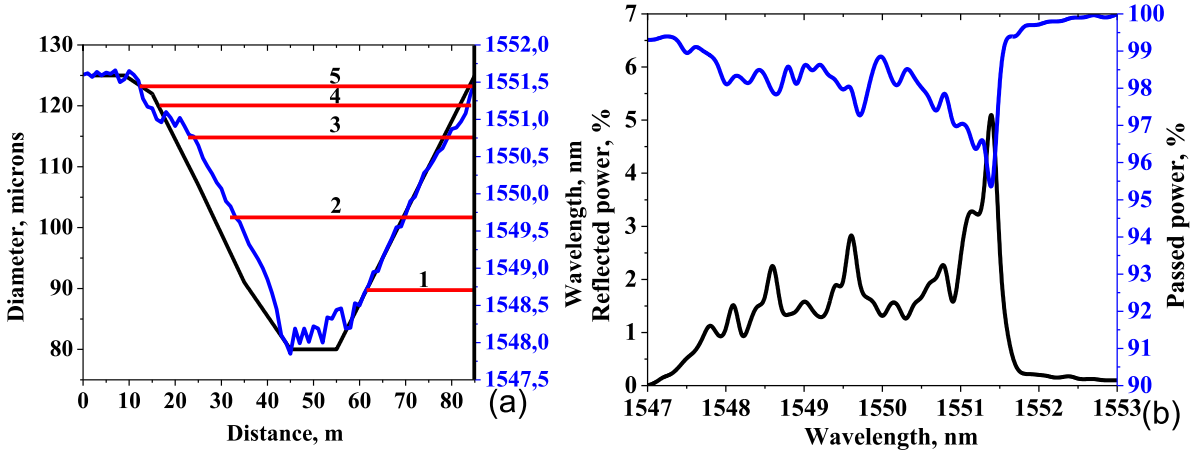

Fig. 1. (a) Tapered FBG fiber profile of the outer diameter (black) and the peak reflectivity wavelength (blue) (a) Total fiber reflection (black) and transmission (blue) spectra (b). The length of the Brillouin laser cavity at different pumping wavelengths are shown by red lines. (For interpretation of the references to colour in this figure legend, the reader is referred to the web version of this article.)

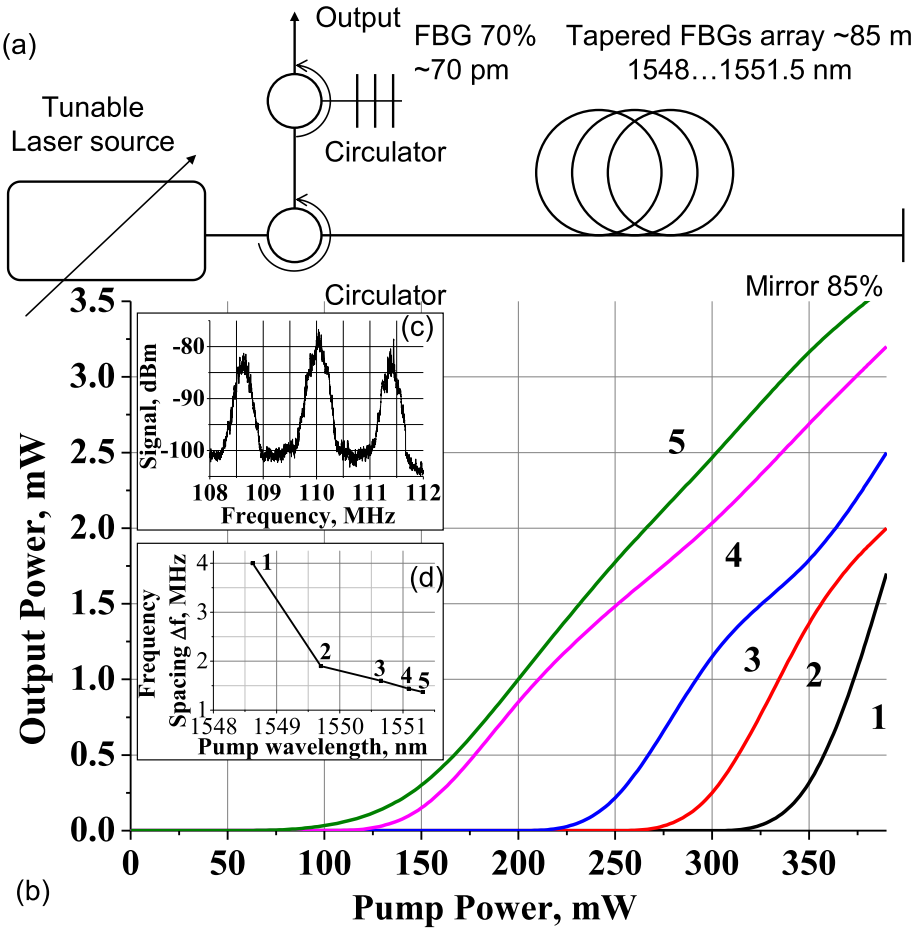

Fig. 2. Brillouin laser configuration (a); power laser characteristics as a dependence of different pumping wavelengths (b); a typical self-heterodyne RF laser spectrum recorded at the pump wavelength of 1551.31 nm (c) and the dependence of the frequency spacing Δf from the pumping wavelength (d). The pumping wavelengths are 1548.62 nm, 1549.7 nm, 1550.65 nm, 1551.09 nm, 1551.31 nm – curves 1–5, respectively.

configuration comprising new optical fiber structure highlights an advance of new fiber technology for Brillouin laser applications.

Acknowledgments

The research was supported by the Russian Fund of Basic Researches (16-32-60109 mol_a_dk, 16-42-732135 R-OFIM) and Ministry of Education and Science of Russian Federation (14. Z50.31.0015, 16.3788.2017/4.6 and 16.4959.2017/6.7). A.F. acknowledges a support from the Leverhulme Trust (Visiting Professor, Grant ref: VP2-2016-042).

References

[1] Fotiadi AA, Brambilla G, Ernst T, Slattery SA, Nikogosyan DN. TPA-induced long-period gratings in a photonic crystal fiber: inscription and temperature sensing properties. J Opt Soc Am B 2007;24:1475–81.
[2] Caucheteur C, Fotiadi AA, Mégret P, Slattery SA, Nikogosyan DN. Polarization properties of long-period gratings prepared by high-intensity femtosecond 352-nm pulses. IEEE Photon Technol Lett 2005;17:2346–8.
[3] Wang C, Yao J. Fiber Bragg gratings for microwave photonics subsystems. Opt. Express 2013;21:22868–84.
[4] Liu X, Wang T, Wu Y, Gong Y, Rao Y-J. Dual-parameter sensor based on tapered FBG combined with microfiber cavity. IEEE Phot Techn Lett 2014;26:817–20.
[5] Chryssis AN, Lee SM, Lee SB, Saini SS, Dagenais M. High sensitivity etched core fiber Bragg grating sensors. IEEE Phot Technol Lett 2005;17:1253–5.
[6] Zaitsev IA, Butov OV, Voloshin VV, Vorobev IL, Vyatkin MYu, Kolosovskii AO, Popov SM, Chamorovskii Yu K. Optical fiber with distributed bragg type reflector. J. Commun. Technol. Electron. 2016;61:639–45.
[7] Chamorovskiy Yu K, Butov OV, Kolosovskiy AO, Popov SM, Voloshin VV, Vorobev IL, Vyatkin M Yu. Metal-Coated Bragg grating reflecting fibre. Opt Fiber Technol 2017;34:30–5.
[8] Soller B, Gifford D, Wolfe M, Froggatt M. High resolution optical frequency domain reflectometry for characterization of components and assemblies. Opt. Express 2005;13:666–74.
[9] Faustov AV, Gusarov A, Liokumovich LB, Fotiadi AA, Wuilpart M, Mégret P. Comparison of simulated and experimental results for distributed radiation-induced absorption measurement using OFDR reflectometry. Proc SPIE 2013;8794:879430.
[10] Faustov A, Gussarov A, Wuilpart M, Fotiadi AA, Liokumovich LB, Kotov OI, Zolotovskiy IO, Tomashuk AL, Deschoutheete T, Mégret P. Distributed optical fibre temperature measurements in a low dose rate radiation environment based on Rayleigh backscattering. Proc SPIE 2012;8439:84390C.
[11] Faustov AV, Gusarov AV, Mégret P, et al. Tech Phys Lett 2015;41:414.
[12] Faustov AV, Gusarov AV, Mégret P, et al. Application of phosphate doped fibers for OFDR dosimetry. Results Phys. 2016;6:86–7.
[13] Popov SM, Chamorovsky YuK, Mégret P, Zolotovskii IO, Fotiadi AA. Brillouin random lasing in artifice rayleigh fiber. European Conference on Optical Communication (ECOC) 2015;1–3.
[14] Popov SM, Chamorovski YK, Isaev VA, Mégret P, Fotiadi AA, Zolotovskii IO. Electrically tunable Brillouin fiber laser based on a metal-coated single-mode optical fiber. Results Phys. 2017;7:852–3. ISSN: 2211-3797.
[15] Fotiadi AA, Lobach I, Mégret P. Dynamics of ultra-long Brillouin fiber laser. Proc SPIE 2013;8601. 86011K.